Cr-based MOCVD layers as conducting diffusion barriers for copper metallization

F. Maury, F.D. Duminica, C. Gasqueres,
Centre Interuniversitaire de Recherche et d'Ingénierie des Matériaux, ENSIACET,
118 route de Narbonne, 31077 Toulouse cedex 4, France.

Two types of amorphous Cr-based thin films, CrC_xN_y and $CrSi_xC_y$, were grown by low pressure MOCVD on Si substrates using respectively $Cr(NEt_2)_4$ and $Cr[CH_2SiMe_3]_4$ as single-source precursor in the low temperature range 400-420 °C and 475-500 °C. Their properties as conducting diffusion barrier against Cu were investigated and the results are discussed. $CrSi_xC_y$ exhibits a better thermal stability and a good Cu wettability but a high resistivity, which is detrimental for this application. CrC_xN_y has a low resistivity, a satisfactory stability up to 650 °C without undesirable interfacial reactions and an excellent conformality.

Keywords: MOCVD; CrC_xN_y films; $CrSi_xC_y$ films; Diffusion barriers; Cu metallization;

I. INTRODUCTION

In increasing efforts to reduce the dimensions of integrated circuits, copper is used as interconnect material in replacement of aluminum and its alloys. However, because Cu significantly diffuses in Si, SiO_2 and low-k dielectrics, a diffusion barrier is required to avoid the degradation of the electrical contacts. Obviously, there are stringent requirements for these conducting thin films as well as for their deposition processes. In order to fulfill these multi-functions, an ideal barrier diffusion must satisfy the requirements presented in table I.

Table I: properties of an ideal diffusion barrier

Material Criteria
• High melting point
• High atomic density
• Low resistivity *(< 1000 μΩ.cm)*
• Amorphous structure *(or nanocrystalline)*
• Good thermal stability (*500 °C*)
• Inert with Cu and other materials (*Si, SiO_2*)
• Adhesion promoter for Cu (*good wettability*)
Process Criteria
• Low temperature deposition
• Control of nanometric thicknesses
• Excellent conformality (low pressure)
• Deposition process compatible with microelectronic fabrication techniques

Different materials and their performance evaluation were reviewed in a previous paper [1]. Thus, the first conducting materials that were studied as barriers are compounds with a high melting point like (*i*) refractory metals [2-4], (*ii*) their alloys [5], and (*iii*) the transition metal nitrides [6-8]. Indeed, these materials are well known for their good thermal and chemical stability, and for their relatively low electrical resistivity. One of the solutions to deposit amorphous materials characterized by high crystallization temperatures is the addition of hetero-elements in transition metal nitrides as metalloid elements (B, C or Si) to form mixed nitrides. Currently, the efforts focus on the ternary compounds of the type M-Si-N (M = Ti, Ta, W), which exhibit interesting properties [9, 10].

The thermodynamic prediction of the reactivity of transition metals revealed that the elements of the group V (V, Nb, Ta) and VI (Cr, Mo, W) are stable with copper [11].

Cr-based layers can be deposited at low temperature by Metal-Organic Chemical Vapor Deposition (MOCVD). The use of metalorganic precursors allows significant decrease of the deposition temperature compatible with the microelectronic fabrication technique. In addition, the use of low pressure MOCVD allows the growth of very thin films with good step coverage on high aspect ratio patterns. Thus, various CrN_xC_y films can be deposited in the Cr-N-C ternary system using metal-organic precursors, in particular a ternary metastable compound $Cr_3(C_{0.8}N_{0.2})_2$ as shown in fig 1 a) [12]. Amorphous thin films of this ternary compounds can be deposited by MOCVD using $Cr(NEt_2)_4$ as single-source precursor [12, 13].

Among the ternary systems, it is known that addition of silicon in transition metals nitrides to form M-Si-N phases increases considerably their crystallization temperature and provides high performance barriers. As a result, in parallel to the Cr-N-C system above mentioned, we were also interested by the Cr-Si-C system to find new barrier materials. In this family of ternary compounds, we have previously deposited by MOCVD amorphous $CrSi_xC_y$ films using $Cr(CH_2SiMe_3)_4$ as single-source precursor [14]. Similarly with the Cr-C-N system, we were particularly interested by the ternary metastable compound Cr_5Si_3C (namely the τ phase in fig. 1 b).

Preliminary results obtained in this cold-wall reactor were recently reported separately for the growth of CrN_xC_y [15] and $CrSi_xC_y$ [16]. In this paper, details on these processes are described and the behavior of these Cr-based thin films as barrier materials is compared and discussed.

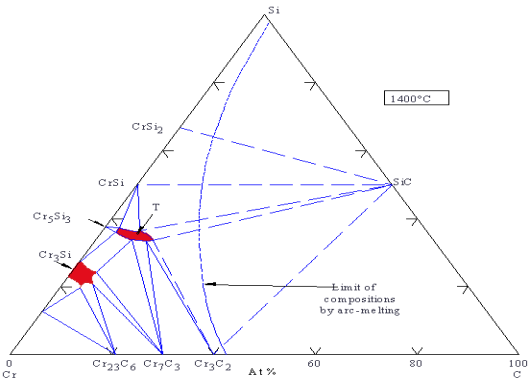

Fig.1: Isothermal Cr-N-C and Cr-Si-C diagrams showing the ternary compounds that could be deposited.

II. EXPERIMENTAL METHODS

II.1 MOCVD process

The growth was carried on in a cold-wall, vertical quartz MOCVD reactor (fig. 2). The deposition processes are described elsewhere [17] and the deposition conditions are summarized in Table II.

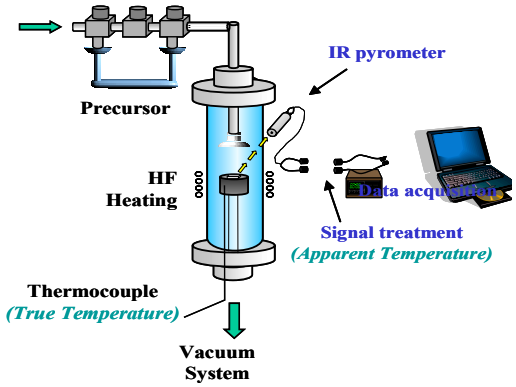

Fig. 2: Sketch of the MOCVD reactor

Table II: Typical growth conditions of the barriers

Precursor	$Cr(NEt_2)_4$	$Cr(CH_2SiMe_3)_4$
Growth Temperature (°C)	400 - 420	475 - 500
Total Pressure (Torr)	0.1	0.5
Carrier Gas (sccm)	H_2 (5)	He (10)
Vaporization Temperature (°C)	50	35 - 38
Mole Fraction	$9.9\ 10^{-3}$	$2.8\ 10^{-3}$
Precursor flow rate (sccm)	0.05	0.027

Si(100) and thermal silica 500 nm thick (SiO_2/Si) wafers were used as substrates. The step coverage of barrier films was investigated on patterned SiO_2(750 nm)/Si substrates in trenches with aspect ratios (AR = height/width) in the range 0.1 to 3. For the evaluation of the diffusion barrier properties, approximately 400 nm thick Cu films were deposited in a cold-wall stainless steel CVD reactor using $Cu(thd)_2$ as precursor on 60-300 nm thick Cr-based barriers. The typical Cu growth conditions were presented elsewhere [18]. After Cu metallization, the samples were cured at 250 °C for 30 min in H_2 ambient to reduce Cu_2O traces, which could be formed during Cu deposition due to the presence of oxygen in the thd ligands (thd = $C_{11}H_{19}O_2$; 2,2,6,6-tetramethyl-3,5-heptanedionate). Then, the Cu/barrier/Si structures were annealed in the temperature range 550-750 °C under atmospheric pressure of H_2 for 30 min in the MOCVD reactor used for the growth of the barriers.

II.2 Properties of the molecular precursors

The molecular structure of precursor $Cr(NEt_2)_4$ and $Cr(CH_2SiMe_3)_4$ are shown in table III. In $Cr(NEt_2)_4$ the chromium atom is bonded to four nitrogen atoms of alkylamido groups. It is a green and viscous liquid at room temperature. It is air sensitive and must be handled under controlled atmosphere in a glove box. It is sufficiently volatile, ~$3x10^{-3}$ Torr at 60 °C [12], to be vaporized at 50 °C and transported using a carrier gas into the reactor under reduced pressure. From measurements of the weight loss of the bubbler after CVD runs for different periods, we have determined a mean evaporation rate of 0.76 $mg.min^{-1}$. This typical value corresponds to a molecular flow rate of 2.24 $\mu mol.min^{-1}$ or 0.05 sccm. The vaporization rate is approximately constant until 500 min when a single bath is used in the thermostated bubbler.

In $Cr(CH_2SiMe_3)_4$ the chromium atom is bonded to four carbon atoms. Its melting point is relatively low (39-40 °C), and it has a sufficient volatility ($5.2x10^{-3}$ Torr/25 °C [14]) to be vaporized and transported in the gas phase using a saturator and a carrier gas. It is also particularly sensitive to oxygen and moisture and, as a result, it was handled in a glove box under argon atmosphere. At 38 °C the sublimation rate was found constant for more than 11 h using only one filling of the saturator. Beyond this period, the sublimation rate decreases. Typically the sublimation rate is 0.48 $mg.min^{-1}$, which corresponds to a molecular flow rate of 1.20 $\mu mol.min^{-1}$ or 0.027 sccm.

Table III : Physical properties, schematic structure and vaporization rate of the chromium precursors: a) $Cr(NEt_2)_4$; b) $Cr(CH_2SiMe_3)_4$

a) 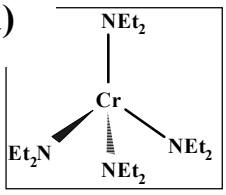	• **Green liquid** • **Air sensitive** • **Stable < 100 °C *(ATG)*** • **3 10^{-3} Torr / 60 °C** • **2.24 µmol.min^{-1}**	**b)** 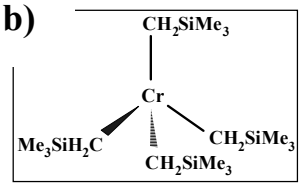	• **Crystalline pouder** • **Air sensitive** • **m.p. = 39 °C** • **5.2 10^{-3} Torr / 25 °C** • **1.20 µmol.min^{-1}**

III. RESULTS AND DISCUSSION

III.1 Structure and morphology

As-deposited CrC_xN_y and $CrSi_xC_y$ films exhibit amorphous structure. Annealing under H_2 during 30 minutes of CrC_xN_y layer leads to the crystallization starting from 700 °C to form the orthorhombic phase $Cr_3(C_{0.8}N_{0.2})_2$ as shown in fig 3a). $CrSi_xC_y$ are more stable since their structure does not change for annealing until 850 °C for few hours (fig 3b). As expected, this is likely due to the incorporation of silicon into the films, which contributes to the amorphization.

The two types of Cr-based barriers are very compact and no grains were observed on SEM micrographs. This is noteworthy because grain boundaries are generally a preferential diffusion path. SEM observations have shown the highly smooth surface morphology of the two types of layers. Their structure is very dense. Figure 4 shows the good conformality of the Cr-based barriers. The lateral step coverage of CrC_xN_y films for trenches with aspect ratio (AR) = 1.5 is 77 % while the bottom step coverage is higher than 70 %. As frequently observed, the step coverage tends to decrease by increasing AR. For instance, the bottom step coverage is 61 % for AR = 2.4. For $CrSi_xC_y$ films, the uniformity of the step coverage is less good. For instance, sidewall coverage in trenches with aspect ratio 1.5 is only 44 % while the bottom step coverage is 60 %. By contrast with CrN_xC_y, nodule formation is observed for $CrSi_xC_y$ in small features on the upper corner of the contact. This overhang profile near the top and poor step coverage at the bottom corner may cause localized failure of the barrier [18].

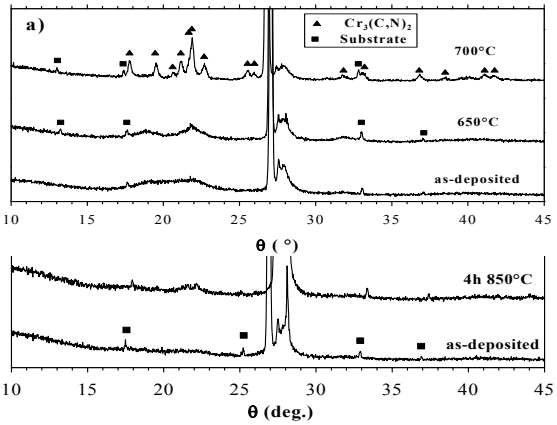

Fig. 3: Grazing incidence (2 deg) XRD patterns of : a) CrC_xN_y(190 nm)/SiO_2/Si samples after annealing at 650 and 700 °C for 30 min under H_2 atmosphere; b) $CrSi_xC_y$ layers after annealing under H_2 atmosphere at 850 °C during 4 h. The group of peaks around 27-28 deg originates from the substrate.

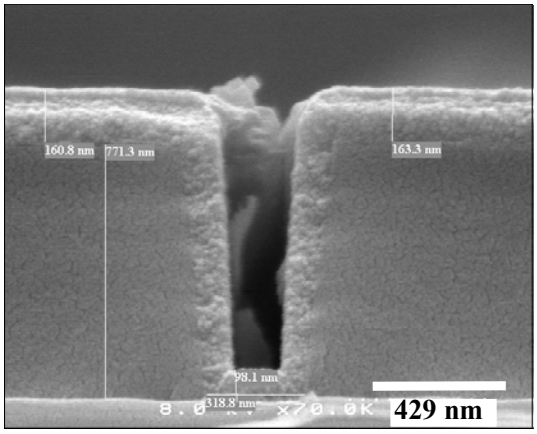

Fig. 4: FEG-SEM micrograph showing the conformality of CrC_xN_y thin films grown on patterned SiO_2/Si substrates. The aspect ratio of the trenches is respectively 2.4.

III.2 Resistivity

The electrical resistivity of CrC_xN_y films increases by decreasing the film thickness. This was due to the presence of an oxidized interphase which played a dominant role in the thinner films. After an improvement of the process in the early stages of the growth, especially after in situ analyses by IR pyrometry [19], this was overcome and the resistivity was typically lower than 1000 μ□.cm even for thicknesses of 25 nm. The resistivity of as-deposited CrC_xN_y films grown at 420 °C on SiO_2/Si substrates is typically 550 μ□.cm and is not affected by annealing under H_2 atmosphere until 650 °C (fig 5 b). Above this temperature, the resistivity decreases suddenly to 150 μ□cm because of the crystallization of the films (Fig 3a). The resistivity of CrC_xN_y films annealed at 550 °C, which is just below the crystallization temperature, increases slightly after 30 min from 550 to 600 μ□.cm, then remains stable for at least 6 h (fig. 5a). This reveals a good behavior of this thin film material at this temperature. The slight increase of the resistivity during the early stages of this annealing treatment is likely due to the transition of the quasi amorphous structure of as-deposited films to a nanocrystalline structure.

The resistivity of as-deposited $CrSi_xC_y$ films decreases of almost three orders of magnitude by increasing the deposition temperature from 400 to 500 °C to reach 10^5 μ□cm at 475 °C.

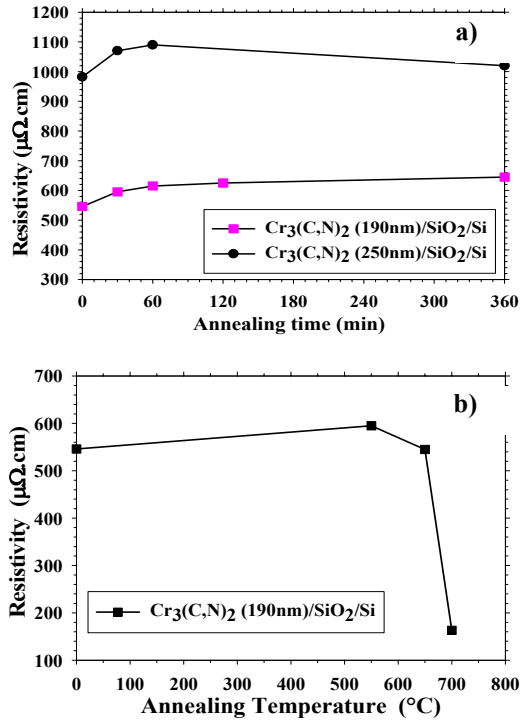

Fig 5: Influence of the annealing conditions under H_2 atmosphere on the resistivity of $Cr_3(C,N)_2$ (190 nm)/SiO_2/Si samples: (a) effect of the annealing time at 550 °C; (b) effect of the annealing temperature (time = 30 min);

III.3 Copper wettability

The surface morphology of Cu films deposited on the two types of barrier is different. When the growth occurs on CrC_xN_y the Cu films are constituted of small (200-300 nm), monodisperse and disjointed grains leading to a relatively high porosity (Fig. 6a). For those deposited on $CrSi_xC_y$ we observe larger grains and a better coalescence giving a higher compactness (Fig. 6b). The surface morphology of Cu and the lower value of water contact angle, 82 deg for $CrSi_xC_y$ compared to 96-108 deg for CrC_xN_y, respectively, indicate that $CrSi_xC_y$ surface is the most hydrophilic. The presence of Si in the barrier layer certainly increases the surface density of adsorbed polar groups as OH emerging from the surface, which enhance the heterogeneous decomposition of the precursor $Cu(thd)_2$ and facilitates the nucleation and the growth of Cu.

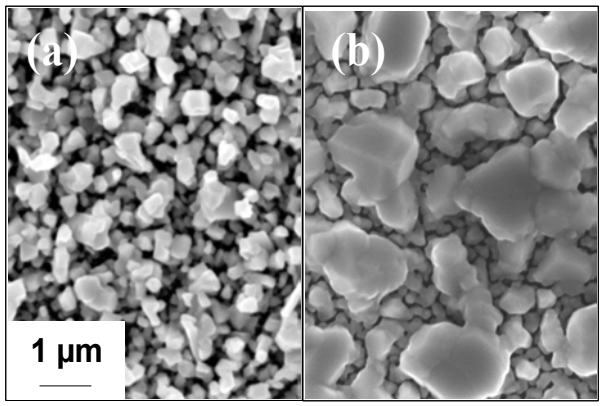

Fig 6: Surface morphology of MOCVD Cu films (□ 400 nm thick) grown on (a) CrC_xN_y and (b) $CrSi_xC_y$ barrier.

III.4 Behavior of Cu/Barrier/Si structures

Direct SIMS profiles through Cu/barrier/Si structures do not give fruitful informations about Cu diffusion through the barrier because of secondary effects as Cu implantation during the sputtering for the profile analysis. Thus, after annealing treatments, the Cu films of the Cu/barrier/Si structures were entirely removed using an etching solution (diluted HNO_3). Then, the samples were rinsed in distilled water, dried under N_2 stream and analyzed by SIMS.

The relative level of Cu analyzed in the barrier depends on the annealing temperature. For instance, after annealing at 700 °C the Cu level in $CrSi_xC_y$ barrier is approximately two orders of magnitude higher than in as-deposited structure (Fig. 7). For a series of annealing treatments of Cu/$CrSi_xC_y$/Si structures, the Cu/Cr intensity ratio measured after Cu chemical etching at a depth of approximately 25

nm in the barrier (vertical dotted line in fig. 7) increases sharply for annealing temperatures higher than 650 °C. This reveals a significant diffusion of Cu through the $CrSi_xC_y$ barrier. This is in good agreement with XRD data since the formation of Cu_3Si was detected around 700 °C [17].

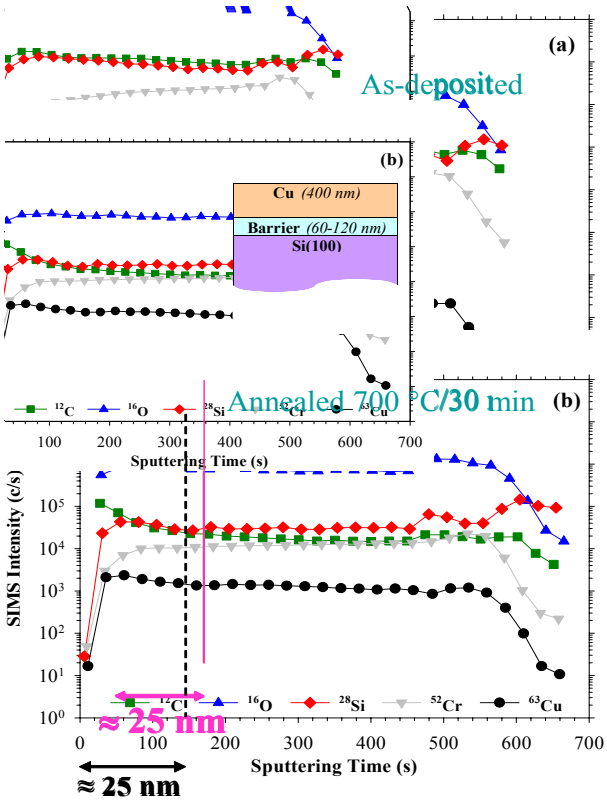

Fig. 7: SIMS depth profiles of $Cu/CrSi_xC_y/Si$ structures after removal of the Cu film by chemical etching prior to SIMS analyses: (a) as-deposited and (b) after annealing at 700 °C for 30 min in H_2 ambient.

IV. CONCLUSION

Two types of amorphous Cr-based thin films, CrC_xN_y and $CrSi_xC_y$, were grown at low temperature by MOCVD on Si substrates. Their properties as conducting diffusion barrier against Cu were investigated. $CrSi_xC_y$ exhibits a better thermal stability and a good Cu wettability but a high resistivity, which is detrimental for this application. CrC_xN_y has a low resistivity, a satisfactory stability up to 650 °C without undesirable interfacial reactions and an excellent conformality.

Compared to literature data recently reviewed [1], the performances of CrC_xN_y layers are very promising (fig. 8). As mentioned in a recent paper [18], the key point is to control carefully the growth of ultra-thin layers with negligible oxygen contamination.

Improvement of our MOCVD reactor and plasma post-treatment are possible solutions currently under investigation. Then, further tests will be carried out to evaluate the properties of ultra-thin CrC_xN_y barrier, which is already regarded as a very good candidate.

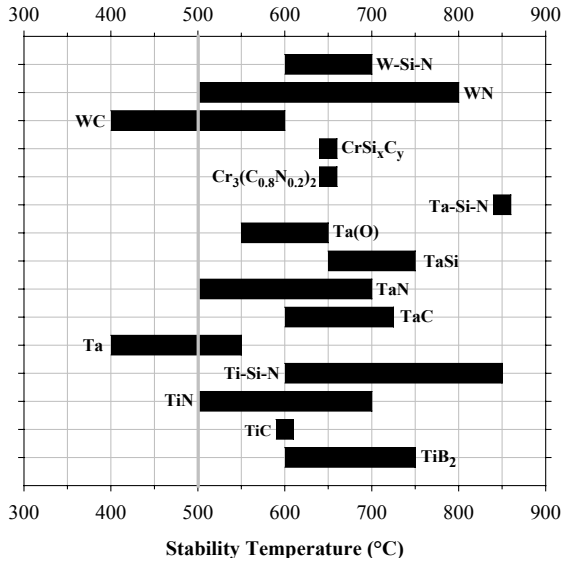

Fig. 8: Stability range of various materials used as Cu diffusion barriers. The temperature of 500 °C is considered as the minimum temperature stability.

[1] C. Gasquères, F. Maury, Trends in Vacuum Science & Technology,. 6 (2004) 109.
[2] W.-F. Wu, K.-L. Ou, C.-P. Chou, and C.-C. Wu, J. Electrochem. Soc., 150(2), (2003) G83.
[3] Y. Ezer, J. Härkönen, V. Sokolov, J. Saarilahti, J. Kaitila, and P. Kuivalainen, Mat. Res. Bull., 33(9) (1998) 1331.
[4] O. Chyan, T.N. Arunagiri, and T. Ponnuswamy, J. Electrochem. Soc., 150(5), (2003) C347.
[5] S.-Q. Wang, S. Suthar, C. Hoeflich, and B.J. Burrow, J. Appl. Phys., 73(5) (1993) 2301.
[6] S.-H. Kim, D.-S. Chung, K.-C. Park, K.-B. Kim, and S.-H. Min, J. Electrochem. Soc., 146(4) (1999) 1455.
[7] S. Riedel, S.E. Schulz, J. Baumann, M. Rennau, and T. Gessner, Microelectron. Eng., 55 (2001)
[8] C. Marcadal, E. Richard, J. Torres, J. Palleau, L. Ulmer, L. Perroud, J. Piaguet, and G. Rolland, Microelectron. Eng., 37/38 (1997) 197.
[9] M.-A. Nicolet, Appl. Surf. Sci. 91 (1995) 269.

[10] E. Blanquet, B. Chenevier, E. Ramberg, C. Bernard, and R. Madar. in CVD XVI and EUROCVD 14, M. Allendorf, F. Maury, and F. Teyssandier, Editors, PV 08, p. 1212, The Electrochemical Society Proceedings Series, Pennigton, NJ (2003).

[11] C. E. Ramberg, E. Blanquet, M. Pons, C. Bernard, R. Madar, Microelectron.Eng., 50 (2000), 357.

[12] F. Ossola and F. Maury, Chem. Vap. Deposition, 3(3) (1997) 137.

[13] F. Maury and F. Ossola, Applied Organomet. Chem., 12 (1998) 189.

[14] F. Maury, F. Ossola, and F. Schuster, Surf. Coat. Technol., 54-55 (1992) 204.

.

[15] C. Gasquères, F. Maury, CVD XVI/EUROCVD 14; M. Allendorf, F. Maury, and F. Teyssandier, Editors, PV 08, p. 1255, The Electrochemical Society Proceedings Series, Pennigton, NJ (2003). 213

[16] D. F. Duminica, F. Maury, CVD XVI/EUROCVD 14; M. Allendorf, F. Maury, and F. Teyssandier, Editors, PV 08, p. 1247, The Electrochemical Society Proceedings Series, Pennigton, NJ (2003).

[17] C. Gasquères, F.-D. Duminica, F. Maury and F. Ossola, J. Electrochem. Soc., 152 (2005) G651.

[18] C. Gasquères, F.-D. Duminica, F. Maury, J. Electrochem. Soc., 152 (2005) G907.

[19] C. Gasqueres, F. Maury, and F. Ossola, Chem. Vap. Deposition, 9(1) (2003) 34.